Available online at www.sciencedirect.com
SCIENCE DIRECT®
ELSEVIER
Surface and Coatings Technology xx (2003) xxx–xxx
SURFACE & COATINGS TECHNOLOGY
www.elsevier.com/locate/surfcoat

Preparation of magnetron sputtered TiN_xO_y thin films

F. Vaz[a,*], P. Cerqueira[a], L. Rebouta[a], S.M.C. Nascimento[a], E. Alves[b], Ph. Goudeau[c], J.P. Rivière[c]

[a]*Departamento de Física, Universidade do Minho, Campus de Azurém, Guimarães 4800-058, Portugal*
[b]*Departamento de Física, ITN, E.N.10, Sacavém 2685, Portugal*
[c]*Université de Poitiers, Laboratoire de Métallurgie Physique, Futuroscope 86960, France*

Received 5 September 2002; received in revised form 14 February 2003; accepted 22 February 2003

Abstract

Within the frame of this work, r.f. reactive magnetron sputtered TiN_xO_y films were deposited on steel, silicon and glass substrates at a constant temperature of 300 °C. The depositions were carried out from a pure Ti target, under the variation of process parameters such as, the substrate bias voltage and flow rate of reactive gases (a mixture of N_2/O_2). Film colours varied from the glossy golden type for low oxygen contents (characteristic of TiN films) to dark blue for higher oxygen contents. X-ray diffraction (XRD) results revealed the development of a face-centred cubic phase with ⟨111⟩ orientation (TiN type; lattice parameter of approx. 0.429 nm), and traces of some oxide phases. Scanning electron microscopy (SEM) revealed a mixture of very dense and columnar type structures. All these results have been analysed, and are presented as a function of both the deposition parameters and the particular composition, and crystalline phases present in the films.

Keywords: X-ray diffraction; Scanning electron microscopy; Glass substrates

1. Introduction

In the last ten years, an emergent field of research, within the thin film technology, is gaining more and more importance—the so-called decorative coatings. Coloured films on high-quality consumer products, such as eyeglass frames, wristwatch casings and wristbands, are supposed to provide both scratch-resistance and protection against corrosion, while enhancing their appearances, and at the same time lending their surfaces attractive colorations. Regarding the apparent colorations of thin films, one must distinguish between the inherent colorations (e.g. in nitrides, carbonitrides or borides) and apparent colorations, due to the interference effects (e.g. transparent oxide or ultra-thin absorbing films) [1]. Since the apparent colorations of interference films are primarily influenced by thickness [2], their use appears to be less suitable choices as decorative coatings, than the formers. Until now, decorative films are mostly based on elemental materials (Ti, Mo, etc.) and also binary nitrides (TiN, golden yellow; ZrN, greenish yellow; HfN, pale greenish yellow [3]) or titanium carbonitrides [3,4].

The colour tones attainable are, however, largely restricted to these golden yellows, various shades of grey and black [4,5], although some attempts have been made in order to obtain other colours, based on borides, ZrB12 (rosy-red), LaB6 (reddish purple) and YB6 (blue-grey) [5]. The increasing demands for low cost products and reduced material resources, implies that the continuous change in target material, to obtain different coloured films is clearly non-suitable. Taking into consideration that the colours of certain materials (inherent colour), is due to their free electrons from longer wavelengths down to visible region, where they are determined by the selective absorption, commencing at these short wavelengths [5], a new class of materials is gaining importance for these decorative applications, the so-called metal oxynitrides, MeN_xO_y (Me = early transition metal). This importance results from the fact that the presence of oxygen allows the tailoring of film properties between those of 'pure' covalent metal nitride, and those of the largely corresponding ionic oxides. Tuning the oxide/nitride ratio allows one to tune the band-gap, bandwidth, and crystallographic order

*Corresponding author. Tel.: +351-253510471; fax: +351-253510461.
E-mail address: fvaz@fisica.uminho.pt (F. Vaz).

0257-8972/03/$ - see front matter © 2003 Published by Elsevier Science B.V.
doi:10.1016/S0257-8972(03)00416-X

between oxide and nitride, and hence the electronic properties of materials and thus the optical ones, including here the colour.

Nevertheless, the subject is fairly important in terms of industrial application, and thus the public knowledge is very short. Recent publications suggested that the performance of these oxynitrides depends not only on the deposition method, but also on both the concentration and distribution of the nitrogen atoms incorporated into the matrix [6–9]. As far as it is concerned, to our knowledge, these explanations are clearly insufficient, and it is clear from the published works that the knowledge of the fundamental mechanism, which explains the observed behaviour, both structurally and mechanically, is yet insufficient. In fact, a basic understanding of the gas-phase, thin-film oxygen and nitrogen incorporation chemistries, facilitates the processing of oxy- and carbonitrides nanostructures with desirable properties. Taking this into consideration, the main purpose of this work consists of the preparation of coloured films, based on single layered metal oxynitrides, MeN_xO_y (Me = Ti). The relationships between colour and the physical, structural and mechanical properties will be an important goal in this work.

2. Experimental details

TiN_xO_y samples were deposited by reactive r.f. magnetron sputtering from a high purity Ti target (99.731%) onto polished high-speed steel (AISI M2), stainless steel, single crystalline silicon (100) and glass substrates, which were sputter etched (15 min in a pure Ar atmosphere; 200 W r.f. power source). Depositions were carried out in an Ar/N_2+O_2 atmosphere in an Alcatel SCM650 apparatus. The depositions were conducted in rotation mode (substrates were rotating at 60 mm over the target at a constant speed of 4 rpm). The base pressure in the deposition chamber was approximately 10^{-4} Pa and rose to values approximately 4×10^{-1} Pa during depositions. A pure titanium adhesion layer (600 W r.f. power in Ti target, $T_s = 300$ °C and −50 V bias voltage), with a thickness of approximately 0.30 μm, was deposited in each sample, in order to improve the adhesion of the films to the substrates. Substrates were heated to 300 °C and dc biased from −50 V up to grounded state. Two sets of samples were prepared: the first group was prepared with variation of the gas mixture (N_2+O_2) flux, using constant values of temperature (300 °C) and bias voltage (−50 V). Fluxes varied from 3.3 to 16 sccm. Gas mixture partial pressures ranged from 0.02 to 0.05 Pa. Second group was prepared with variation of the bias voltage, a fixed temperature of 300 °C and a constant gas flow of 14 sccm. Depositions were carried out with a constant r.f. power of 2.55 W/cm^2 (800 W) applied to the Ti target. Both sets of samples were prepared with a constant argon flux of 100 sccm.

The atomic composition of the as deposited samples was measured by Rutherford backscattering spectrometry (RBS). Experimental spectra were fitted with the RUMP code [10]. An average number of five 'ball cratering' (BC) experiments were carried out in each sample in order to determine its thickness. X-ray diffraction (XRD) experiments were used for texture characterisation, using a Philips PW 1710 apparatus (Cu K_α radiation).

Colour of the samples was computed from the spectral data, acquired using a hyperspectral imaging system. Samples were illuminated at 8° by radiation, from a Xenon lamp coupled with a tuneable birefringent filter (VariSpec, model VS-VIS2-10HC-35-SQ, Cambridge Research and Instrumentation, Inc, USA), tuneable over the wavelength range 400–720 nm with a half-height full-width of 10 nm at 500 nm. Specular reflected light was acquired with a high-resolution monochrome digital camera (ORCA-ER, Hamamatsu, Japan), with a spatial resolution of 1344×1024 pixels and 12-bit intensity resolution. Measurements were made against the white standard $BaSO_4$ at 10 nm intervals. An area of 3.7×3.7 mm was analysed with a spatial resolution of 12 μm/pixel. Colour specification under the standard CIE illuminant D65 was computed, and represented in the CIELAB 1976 colour space [11,12] for each individual pixel in the area.

3. Results and discussion

3.1. Chemical analysis

The simulations revealed a homogenous composition profile in depth for all layers, which is one of the difficulties in this system due to the high reactivity of oxygen when compared to that of nitrogen [2]. Fig. 1 showed the results obtained for two samples, which are analysed in this work. Tables 1 and 2 presented the composition and thickness of the two groups of samples.

3.2. Structure

Fig. 2a shows the XRD θ/2θ diffraction patterns for samples prepared with variation of gas mixture (N_2+O_2) flow, as well as for reference samples: titanium (for the adhesion layer), titanium nitride (base matrix) and titanium oxide. All these samples were prepared under the same conditions of temperature (300 °C), rotation (4 rpm), polarisation of the substrate (−50 V), power (800 W) and working gas flow (100 sccm). Results revealed a strong dependence of film texture on the percentage of oxygen. The sample with lower percentage of this element (16 at.%) revealed a crystalline structure, which is basically constituted by (111) TiN grains.

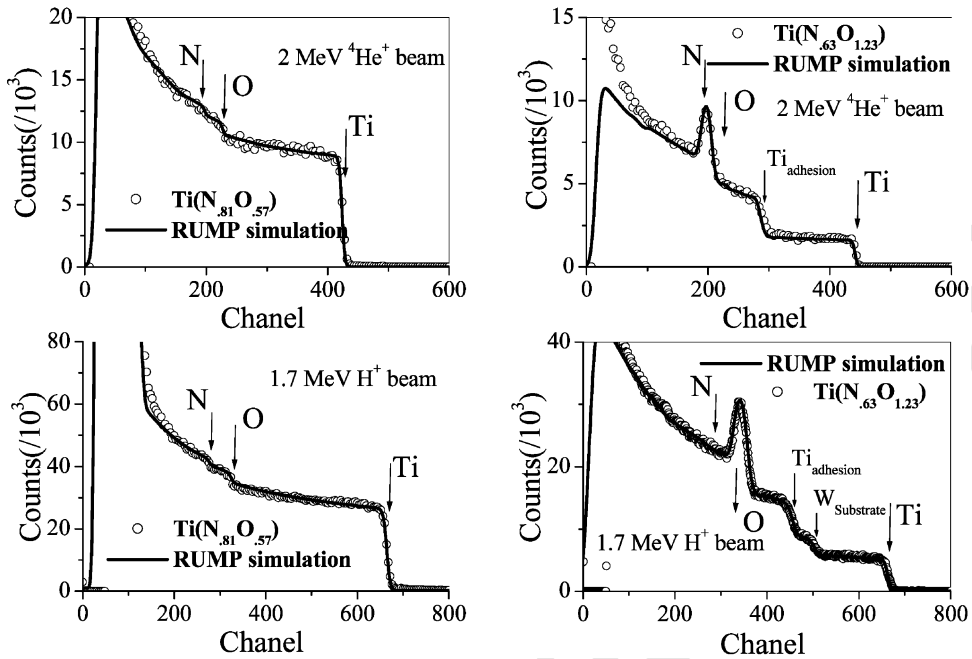

Fig. 1. Rutherford backscattering spectra of 1.7 and 2.0 MeV protons and α-particles, respectively, at normal incidence and scattering angles of 140 and 180°. The full lines represents the RUMP simulations.

The increase of the oxygen percentage is followed by a significant loss of crystallinity, the films with the highest oxygen contents being (34 and 43 at.%), practically amorphous. The reason for this increasing amorphisation of the films is related with the increase of the oxygen content, promoted by the increase in the gas flow (and by the fact that oxygen is much more reactive than nitrogen). The increase of the available oxygen increases dc supersaturation [13], reducing the possibility of crystallisation (mostly that of TiN). The extended deformation of the titanium nitride structure, resulting from the incorporation of oxygen, increases the number of defects, facilitating the amorphisation. In fact, this oxygen doping explains the broadening of the diffraction peaks, as it can be evidenced for intermediate and highest oxygen contents, where the peak broadening is

Table 1
Thickness and composition of the samples prepared with the same bias voltage (−50 V) and variation of the gas mixture flow

Sample	Ti (at.%)	N (at.%)	O (at.%)	$\phi_{mixture(N_2+O_2)}$ (sccm)	Thickness (μm)
Ti (adhesion layer)	100	–	–	–	0.3±0.1
TiN	50±3	50±3	–	$\phi_{N_2}=3.3^*$	1.7±0.2
$Ti(N_{.87}O_{.36})$	45±3	39±3	16±3	10.0	1.1±0.1
$Ti(N_{.81}O_{.57})$	42±3	34±3	24±3	11.5	1.0±0.1
$Ti(N_{.80}O_{.63})$	41±3	33±3	26±3	12.5	1.1±0.1
$Ti(N_{.69}O_{1.17})$	35±3	24±3	41±3	13.5	0.7±0.1
$Ti(N_{.63}O_{1.23})$	35±3	22±3	43±3	14.5	0.9±0. 1
$Ti(N_{.69}O_{.87})$	39±3	27±3	34±3	16.0	0.9±0.1
TiO_2	33±3	–	67±3	$\phi_{O_2}=12^*$	0.8±0.1

* Samples TiN and TiO_2 were prepared with a gas flux of only N and O, respectively.

Table 2
Thickness and composition of the samples prepared with the same gas mixture flow ($\phi_{mixture(N_2+O_2)}=14$ sccm) and variation of the bias voltage

Sample	Ti (at.%)	N (at.%)	O (at.%)	V_{bias} (V)	Thickness (μm)
$Ti(N_{.69}O_{1.17})$	35±3	24±3	41±3	0	2.6±0.2
$Ti(N_{.69}O_{1.17})$	35±3	24±3	41±3	−10	1.2±0.1
$Ti(N_{.78}O_{1.00})$	36±3	28±3	36±3	−30	1.2±0.1
$Ti(N_{.75}O_{.75})$	40±3	30±3	30±3	−50	0.9±0.1

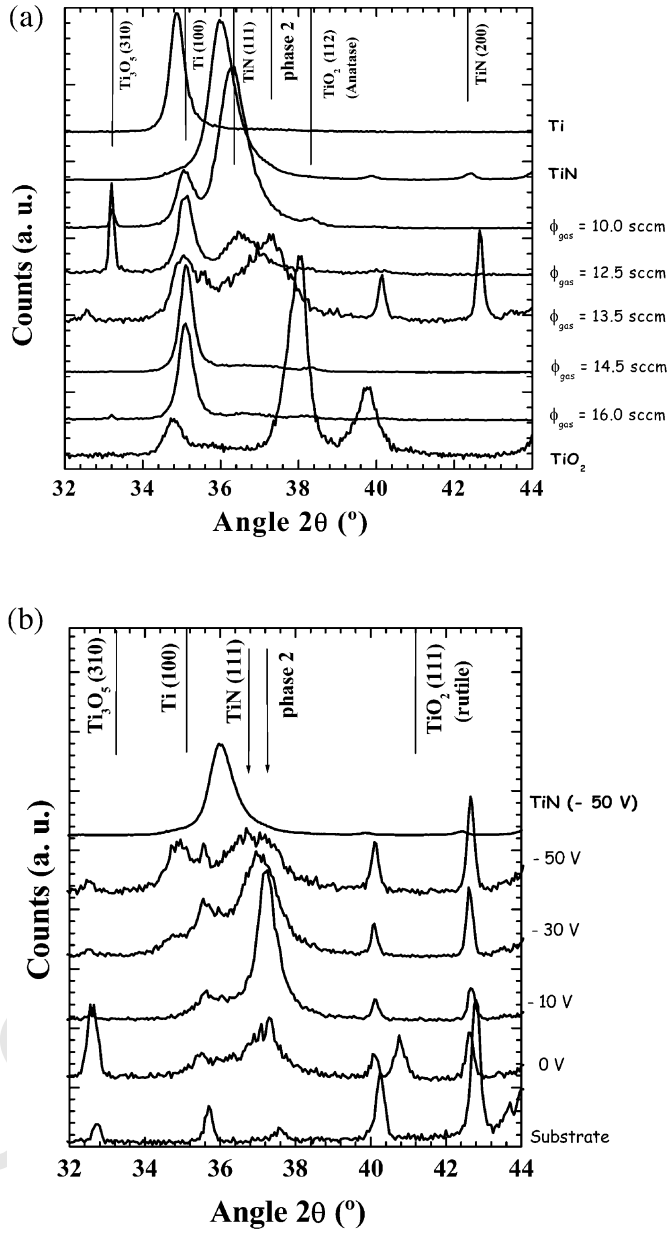

Fig. 2. XRD diffraction patterns of TiN_xO_y films prepared at: (a) constant bias voltage (−50 V), r.f. power (800 W) and different gas mixture flows; and (b) constant r.f. power (800 W), gas flow (14 sccm) and variation in bias voltage: (0, −25, −50, −75 and −100 V).

a clear indication of a mixture of lattice parameters. This mixture of a pure TiN crystalline lattice and also others with oxygen incorporation, which one might call as phase 2, is even clearer in the diffractograms of the samples prepared with different bias voltages (Fig. 2b).

For these samples, and for both the absence (grounded sample) and low ion bombardment cases, the diffraction peak appears at an angular position of approximately 37°, which shifts towards that of TiN with increasing ion bombardment. In fact, at −50 V it is already clear that a mixture of two phases, which would correspond to that of the phase mixture. Although, the doping of TiN matrix with other elements has been claimed in different studies, such as those of Ti–Al–Si–N [14,15], the exact nature of phase 2 is very difficult to be evaluated, but it cannot be matched by any known compound formed with Ti and N, or from various phases of titanium oxide [16].

This fact provides evidence for the possible formation of a titanium, oxygen, nitrogen phase, Ti–O–N, where some of the oxygen atoms are most likely occupying nitrogen positions in the *fcc* TiN lattice. This last assumption has been mentioned in the upper mentioned works [17], but also for recent works concerning (Ta,Si)N coatings [18] in order to explain the XRD results, but no clear experimental evidence was given.

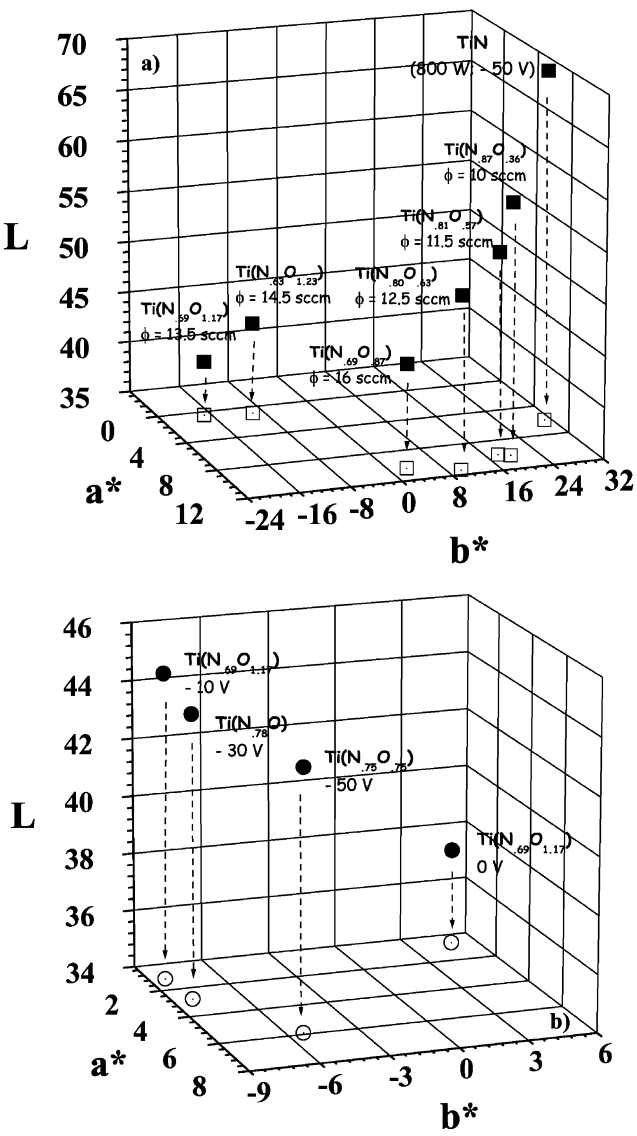

Fig. 3. Average specular colour in the CIELAB 1976 colour space for the samples under the standard CIE illuminant D_{65} and prepared with: (a) different gas flows, and (b) different bias voltages. Open symbols correspond to projections in a^* b^* plane.

Without ion bombardment (see lower diffraction pattern in Fig. 2b), only phase 2 is visible, leading to the conclusion that phase mixing is most likely a consequence of the ion bombardment.

The absence of the ion bombardment and the low deposition temperature (<300 °C) do not provide the necessary mobility for the species that will ensure the complete phase segregation, this being the main reason that explains the formation of this new Ti–O–N structure—phase 2. This phase could be called as a solid solution. Consequently, with increase in the surface mobility, provided by the increase in temperature and/or ion bombardment, phase segregation is enhanced, and thus one can observe the formation of TiN polycrystalline grains, although traces of that Ti–O–N phase are still visible at −50 V. Beyond this main finding of phase mixtures, several reflections corresponding to Ti–O structures were also indexed. These structures also tend to disappear with the increase in the oxygen content, which is again a consequence of the difficulty in growing 'pure' structures with the gas mixture.

Table 3
CIE 1976 $L^*a^*b^*$ space colour coordinates for samples prepared with the same bias voltage (−50 V) and variation of the gas mixture flow. The colour variation for each sample is represented by ±1/2 S.E.M. (standard error of the mean) across an area of 3.7×3.7 mm analysed with a spatial resolution of 12 μm/pixel

Sample	Gas flow	L^*	a^*	b^*
TiN	$\phi_{N_2}=3.3$	69.2±3.5	6.0±1.6	30.9±1.2
$Ti(N_{.87}O_{.36})$	10.0	59.5±3.1	10.2±4.5	19.6±3.4
$Ti(N_{.81}O_{.57})$	11.5	54.6±1.9	9.9±1.9	18.0±1.9
$Ti(N_{.80}O_{.63})$	12.5	51.8±1.7	11.4±1.2	10.1±1.1
$Ti(N_{.69}O_{1.17})$	13.5	40.3±2.7	0.5±2.4	−17.1±1.2
$Ti(N_{.63}O_{1.23})$	14.5	43.9±2.3	0.9±2.9	−9.8±2.5
$Ti(N_{.69}O_{.87})$	16.0	45.1±1.1	10.4±0.9	2.8±0.8

3.3. Colour characterisation

Fig. 3a and Table 3 show the average specular colour, represented in the CIELAB 1976 colour space [11,12], for each of the samples prepared with variation in the reactive gas mixture flow. In Table 3 the colour variation for each sample is represented by ±1/2 S.E.M. (standard error of the mean) across an area of 3.7×3.7 mm analysed with a spatial resolution of 12 μm/pixel. It can be seen that low oxygen contents produces a bright yellow-pink colour, which gradually shifts to dark golden yellow as its contents increases. For larger contents of oxygen, the colour produced was dark blue.

Fig. 3b and Table 4 show the average specular colour for each of the samples prepared with the same gas mixture flow ($\phi_{mixture(N_2+O_2)}=14$ sccm), and variation of the bias. In the table, the colour variation for each sample is represented by ±1/2 S.E.M. (standard error of the mean) across an area of 3.7×3.7 mm analysed with a spatial resolution of 12 μm/pixel.

Low negative voltages produced bluish colours, which was shifted towards a whiter metallic as the absolute

Table 4
CIE 1976 $L^*a^*b^*$ space colour coordinates for samples prepared with the same gas mixture flow ($\phi_{mixture(N_2+O_2)}=14$ sccm) and variation of the bias voltage. The colour variation for each sample is represented by ±1/2 S.E.M. (standard error of the mean) across an area of 3.7×3.7 mm analysed with a spatial resolution of 12 μm/pixel

Sample	Bias (V_b)	L^*	a^*	b^*
$Ti(N_{.69}O_{1.17})$	0	37.3±2.6	0.7±2.4	4.9±1.3
$Ti(N_{.69}O_{1.17})$	−10	44.6±2.4	1.2±2.6	−8.3±1.7
$Ti(N_{.78}O_{1.00})$	−30	43.8±2.2	2.8±2.5	−8.1±0.6
$Ti(N_{.75}O_{.75})$	−50	43.0±2.0	5.9±1.6	−5.3±1.6

value of the voltage increased. These results indicated that not only composition, but also the bias voltage significantly influenced the colour of the coating. In fact, these results also indicated that it is possible to produce very different decorative coatings, only by varying the gas flow mixture and keeping the experimental conditions of the bias voltage constant, at the sputtering target. Furthermore, a careful observation of the results in both the graphs shows that even equal compositions can develop significantly different colours, as in the case of the $Ti(N_{.69}O_{1.17})$ sample. The two samples with this same composition (that of graph in Fig. 3a prepared with 13.5 sccm gas flux and −50 V bias, and that of graph in Fig. 3b prepared with 14 sccm and 0 V bias voltage) revealed very different colours, the negatively biased sample being dark blue, while the unbiased developed a white metallic colour. Moreover, −10 V bias samples (Fig. 3b) also have the same composition, but the colour is also tending for blue.

These results indicate that composition, although important, is not certainly the main parameter in coating colour variation. On the other hand, ion bombardment seems to be much more important for this colour variation, which induces the conclusion that the different structures and film growth conditions are significantly influencing the colour results. This can be easily seen in Fig. 2b, where the samples prepared with 0 V and −10 V, although with the same composition as mentioned before, developed very different microstructures. The difference is correlated with the presence of that referred phase 2, which is particularly evident in the biased sample ($V_b = -10$ V). In fact, the presence of this phase revealed by the diffraction peak at ∼37° is influencing significantly the coating colour. A closer look at both the plots of Fig. 2a and b, shows that samples prepared at −10 and −30 V (Fig. 2b), together with that prepared at −50 V, with a gas flow of 13.5 sccm have clearly developed this phase, and all the results were revealed in dark blue colour.

Furthermore, the −50 V sample of Fig. 2b also has some traces of this phase, although the phase segregation promoted by the ion bombardment is already present. Again, the colour of this sample is slightly blue. The clear appearance of the TiN phase (golden) in this sample is shifting its colour towards a more yellowish tone. The samples with a clear TiN phase (although with traces of oxygen doped phases, seen by the peak broadening) developed a gold-brown colour, which is consistent with that of TiN. These results indicated that the microstructure, influenced primarily by the preparation conditions, namely ion bombardment, was ruling the coating colour, which in turn induced the conclusion that one can tailor this easily prepared Ti–N–O coating system with the desirable colour.

4. Conclusions

Thin films within the Ti–N–O ternary system were prepared by r.f. reactive magnetron sputtering. All the samples were prepared with a constant r.f. power (800 W–2.55 W/cm^2) at the Ti elemental target. Colour variation was obtained by varying the N_2+O_2 gas mixture and bias voltage. Structural characterisation results revealed a strong dependence of the film texture on the percentage of oxygen. The sample with lower percentage of this element (16 at.%) reveals a crystalline structure, which is basically constituted by (111) TiN grains. A significant loss in crystallinity, the films with the highest oxygen contents, being amorphous, follows the increase of the oxygen percentage. However, for the intermediate and higher oxygen contents, the diffraction peaks seem to indicate a mixture of lattice parameters.

This mixture of a pure TiN crystalline lattice and others with oxygen incorporation, which one might call as phase 2, is even clearer in the diffractograms of biased samples. For the grounded sample and low ion bombardment, the diffraction peak appears at an angular position of approximately 37°, which shifts towards the TiN, with the increase in ion bombardment. In fact, at −50 V it is already clear that it is a mixture of two phases.

Regarding colour variations, it was observed that for low oxygen contents a bright yellow-pink colour was obtained, which gradually shifted to dark golden yellow as its contents increased. For larger contents of oxygen, the colour produced was dark blue. Variations in the bias voltage revealed bluish colours that shifted towards a whiter metallic, as the absolute value of the voltage increased. These results indicated that beyond composition, microstructure was influenced primarily by the preparation conditions, namely ion bombardment, is the main parameter that rules the coating colour, which induces the conclusion that one can tailor this easily prepared Ti–N–O coating system with the desirable colour.

References

[1] R. Fraunchy, Surf. Sci. Rep. 38 (2000) 195.
[2] M. Ohring, The Materials Science of Thin Films, Academic Press Inc, San Diego, 1992.
[3] E. Budke, J. Krempel-Hesse, H. Maidhof, H. Schussler, Surf. Coat. Technol. 112 (1999) 108–113.
[4] B. Zega, Surf. Coat. Technol. 39/40 (1989) 507.
[5] C. Mitterer, J. Komenda-Stallmaier, P. Losbichler, P. Schmolz, W.S.M. Werner, H. Stori, Vacuum 46 (1995) 1281.
[6] R. Constantin, B. Miremad, Surf. Coat. Technol. 120–121 (1999) 728.
[7] M. Bhat, L.K. Han, D. Wristers, J. Yan, D.L. Kwong, J. Fulford, Appl. Phys. Lett. 66 (1995) 1225.
[8] S.V. Hattangady, H. Niimi, G. Lucovsky, Appl. Phys. Lett. 66 (1995) 3495.

[9] W.L. Hill, E.M. Vogel, V. Misra, P.K. McLarty, J.J. Wortman, IEEE Trans. Electron Devices 43 (1996) 15.
[10] L.R. Doolittle, Nucl. Inst. Meth. B9 (1985) 344.
[11] Colorimetry, CIE Publication, 15, 1971 (Comission Internationale de L'Éclairage).
[12] Recommendations on Uniform Color Spaces, Difference–difference equations, psychometric color terms, CIE Publication, 15 (1978) Suppl. No. 2–70 (Comission Internationale de L'Éclairage).
[13] Y. Imai, M. Mukaida, A. Watanabe, T. Tsunoda, Thin Solid Films 300 (1997) 305.
[14] F. Vaz, Ph.D. Thesis, Minho University, Portugal, 2000.
[15] S. Carvalho, L. Rebouta, A. Cavaleiro, L.A. Rocha, J. Gomes, E. Alves, Thin Solid Films 398–399 (2001) 391.
[16] Powder Diffraction File of the International Center for Diffraction Data, PDF-ICDD cards.
[17] F. Vaz, L. Rebouta, P. Goudeau, T. Girardeau, J. Pacaud, J.P. Riviére, et al., Surf. Coat. Technol. 146–147 (2001) 274, and references therein.
[18] J.W. Nah, S.K. Hwang, C.M. Lee, Mater. Chem. Phys. 62 (2000) 115.